Impact Behaviour of GRP, Aluminium and Steel Plates

L.S. Sutherland & C. Guedes Soares
Centre for Marine Technology and Engineering (CENTEC), Technical University of Lisbon, Instituto Superior Técnico, Lisbon, Portugal

ABSTRACT: Comparative experimental data has been obtained for GRP laminates, and Aluminium 5083 and steel circular fully-clamped plates subjected to lateral impact. The metal plates were much more resistant to perforation than the laminated plates, but the behaviour up to perforation was more complex. A decrease in maximum force and an increase in maximum and final deflections, and absorbed energy was seen when fibre damage of the composite materials became significant. Both composite material and metal plates suffered damage at very low incident energies. However, the composite delamination damage would in practice be much less visible than that for metal plates. Care must be taken to ensure that relevant comparisons are made; flexural stiffness equivalence has been used here, but if strength, thickness, or weight equivalence would have been considered the results would have differed in each case.

1 INTRODUCTION

Three of the main building materials used in the construction of modern small craft are composites, steel and aluminium. Of these, composites are by far the most ubiquitous, almost exclusively as glass reinforced plastic (GRP) in the form of Chopped-Strand Mat (CSM) or Woven Roving (WR) reinforced polyester resin. Metal hull construction uses mild steel or 5000 series aluminium alloys. Wood is also still used, but since there are such a large number of combinations of species and forms and because this is a relatively specialised industry, this material is not considered in the current study.

The main advantages and disadvantages of each material are listed in Table 1 (Gerr 2000, Brewer 1994, Trower 1999, Du Plessis 1996). The numerous advantages of GRP explain to a large extent why it has become so popular. However, a major disadvantage of composites in comparison with metals is the lack of plastic deformation to failure, which means that metal boats are seen as more durable or damage resistant to groundings or collisions.

The susceptibility of composite materials in general to impact damage of has attracted great attention in the literature (Abrate 1998). The authors' previous work (Sutherland & Guedes Soares 1999a, b, 2003, 2004, 2005a, b, c, 2006, 2007) has shown the impact behaviour of GRP to be complex. Internal delamination occurred at very low incident energies, only followed at much higher energies by visible fibre failure leading to penetration and finally perforation. Membrane and bending effects dominated for thinner laminates until back-face fibre damage initiated final failure. Thicker laminates were dominated by shear effects due to delamination, with indentation damage leading to final failure. The response was seen to be dependent on many impact and material parameters.

The aim of this study is to further explore and elaborate on the relative impact performance of GRP, steel and aluminium through an experimental comparison of transversely impacted plates. However, in order to make any meaningful comparisons, a pertinent equivalence between plates of different materials must be selected; e.g. should the plates be of the same thickness, or the same stiffness, or of the same strength? Which criterion is selected will strongly influence the relative performance of the various materials considered, both quantitatively and, in all probability, qualitatively. Here, the approach taken is to consider the case of plates of equivalent bending stiffness.

2 EXPERIMENTAL DETAILS

As representative of the materials used in the marine industry, WR & CSM hand laid-up laminates, structural carbon or 'mild' steel and Aluminium 5083-H111 were considered. The tests on the two laminates were those as reported in previous work (Sutherland & Guedes Soares 2006).

Table 1: Construction materials comparisons

Advantages	Disadvantages
COMPOSITES:	
Lightweight	Little plastic deformation to fail (for impact energy absorption).
Easy to mould complex shapes	
Cheap, more so for series production	Low fire resistance, toxic fumes.
Ability to tailor properties	
No painting or fairing	Production working environment
Low wastage	
No rot or corrosion	
Low maintenance	
Easy to repair	
Non-magnetic	
ALUMINIUM:	
Lightweight	Expensive
Easy to work	Welding distortion
No corrosion	Costly to paint
Non-magnetic	Less readily available
High plastic deformation to fail (for impact energy absorption).	Requires heat insulation
	Electrolysis
	Fatigue
	Less abrasion-resistant
	Can melt at temperatures seen in fires.
STEEL:	
Cheap	Heavy
Simple to fabricate	Hard to Shape
Easy to repair	Welding distortion
Fire resistant	Requires heat insulation
High plastic deformation to fail (for impact energy absorption).	Corrosion
	Electrolysis

An orthophthalic polyester resin was used throughout to laminate 1m square panels by hand on horizontal flat moulds. A fibre mass-fraction of 0.5 and 0.3 (equivalent to fibre volume fractions of approximately 0.35 and 0.2) for WR and CSM plies respectively was stipulated as representative of the values commonly achieved under production conditions in the marine industry. 1, 2 and 3% by mass of accelerator, catalyst and paraffin respectively were added at an ambient temperature of between 18 and 21ºC to cure the resin. In order to ensure sufficient cure, laminates were stored at room temperature for two months before testing.

A plate laterally impacted by a hemi-spherically ended projectile was considered as a commonly studied and relatively severe impact event. In order to make meaningful comparisons the thicknesses of each material were selected to give plate bending stiffness equivalence, using the appropriate WR laminate thickness as the reference value. The closest plate thicknesses available for the metals were used, but since bending stiffness varies as thickness cubed, exact equivalence was not possible (Table 2). However, allowance for these differences was made as discussed in the next section.

Two series of tests were run; 'thin' specimens to induce a bending/membrane controlled event such as would occur at the centre of a panel, and 'thick' specimens to induce a shear/indentation controlled event such as would occur near to a stiffener.

200mm square specimens were cut from the panels and thickness measurements then taken at four points on each specimen prior to testing. Specimen thicknesses are given in Table 2. The specimens were fully clamped between two thick annular circular steel plates of 100mm internal diameter. Four bolts that passed through holes in the clamp plates (and specimen) applied the clamping force.

Table 2: Specimen details

	Thin	Thick
WR:		
Panel Code (No. Plies)	W5	W15
Thickness (mm)	3.17	9.29
Diameter/Thickness	32	11
CSM:		
Panel Code (No. Plies)	C4	C12
Thickness (mm)	3.75 (3.78)*	10.92 (11.06)*
Stiffness : WR Stiffness	-2%	-4%
Diameter/Thickness	27	9
ALUMINIUM:		
Panel Code	AL1	AL2
Thickness (mm)	2.00 (1.82)*	5.92 (5.32)*
Stiffness : WR Stiffness	+33%	+38%
Diameter/Thickness	50	17
STEEL:		
Panel Code	FE1	FE2
Thickness (mm)	1.37 (1.28)*	4.00 (3.74)*
Stiffness : WR Stiffness	+23%	+23%
Diameter/Thickness	73	25

*Thicknesses in parenthesis are those which would give equivalent bending stiffness to the appropriate WR laminate.

Impact testing was performed using a fully instrumented Rosand IFW5 falling weight machine. A small, light hemispherical ended cylindrical projectile (of diameter 10mm for these tests) is dropped from a known, variable height between guide rails onto a clamped horizontally supported plate target. A much larger, variable mass is attached to the projectile and a load cell between the two gives the variation of impact force with time. An optical gate gives the incident velocity, and hence the projectile displacement and velocity and the energy it imparts are calculated from the force-time data by successive numerical integrations. A pneumatic catching device prevents further rebound impacts. Since the projectile is assumed to remain in contact with the specimen throughout the impact event, the projectile displacement is used to give the displacement and velocity of the top face of the specimen, under the projectile. Assuming that frictional and heating effects are negligible the energy imparted by the indenter is that absorbed by the specimen. Thus, this energy value at the end of the test is that irreversibly absorbed by the specimen.

A series of tests were performed for a range of increasing incident energies for each material. Two sets of nominal incident energies were used, one for

'thick' and one for 'thin' specimens. As far as possible exactly the same incident energies were used for all materials but due to guiding rail friction effects this was not always possible, especially at low drop heights. The impact mass was 3.103kg and 4.853kg for the thin and thick specimens respectively.

3 THEORY

As noted in the previous section, it was not possible to arrange plates of the various different materials with exactly the same bending stiffness. Hence, a simplified model is developed here to allow for these differences through normalisation of the various experimental impact responses recorded. The 'ideal' case of a spring-mass model (Abrate 2001) with no damage or membrane or indentation effects will be considered.

This simplified model can also be used as a 'baseline' reference to make useful comparisons between the different material impact behaviours seen. However, the model is not expected to be a good predictor of behaviour since damage occurs even at low incident energies, and membrane and indentation effects are large for thinner and thicker specimens respectively.

The two degree-of-freedom spring-mass model of the impact event, for no damage, is shown schematically in Figure 1.

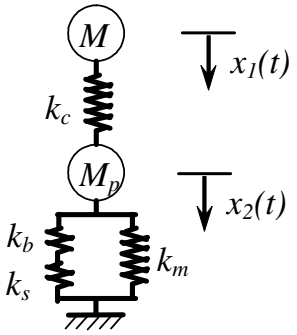

Figure 1. Two degree-of-freedom spring-mass model of impact event.

The bending, membrane, contact and shear stiffness' of the plate are represented by the springs kb, k_s, k_m and k_c respectively. M is the mass of the projectile and Mp that of the plate. The displacements of the projectile and plate are given by the functions of time x_1 and x_2 respectively.

The free body diagrams of M and Mp give the equations of motion,

$$\begin{aligned} M\ddot{x}_1 + F &= 0 \\ M_P\ddot{x}_2 + k_{bs}x_2 + k_m x_2^3 - F &= 0 \end{aligned} \qquad (1)$$

where F is the contact force which is a non-linear function of the indentation,

$$F = f(\alpha) = f(x_1 - x_2) \qquad x_1 > x_2 \qquad (2)$$

When $x_2 > x_1$ the projectile leaves the plate surface and F = 0.

The initial conditions are given by incident impact velocity and that the initial displacements are both zero,

$$\dot{x}(0) = v_i, \qquad x_1(0) = x_2(0) = 0 \qquad (3)$$

The problem must be studied numerically, but assuming indentation and membrane effects are negligible, that shear stiffness is much greater than bending stiffness, and that in comparison to that of the projectile the mass of the plate is very small, leads to a simple one degree of freedom system where $x_1 = x_2 = x$ with the equation of motion,

$$M\ddot{x} + k_b x = 0 \qquad (4)$$

Solving the general solution to (4) using the initial conditions (3) gives,

$$x = v_i\sqrt{\frac{M}{k_b}} \cdot Sin\left(\sqrt{\frac{k_b}{M}} \cdot t\right) \qquad (5)$$

Hence,

$$x_{\max} = v_i\sqrt{\frac{M}{k_b}} \qquad (6)$$

The impact force is now given by that in the spring k_b,

$$F = k_b x = v_i\sqrt{k_b M} \cdot Sin\left(\sqrt{\frac{k_b}{M}} \cdot t\right) \qquad \omega t < \pi \qquad (7)$$

Hence,

$$F_{\max} = v_i\sqrt{k_b M} \qquad (8)$$

The impact duration is given when the projectile leaves the plate at $t = T_c = \pi/\omega$,

$$T_c = \pi\sqrt{\frac{M}{k_b}} \qquad (9)$$

From Young (1989), for a uniform load over a very small central circular area of radius r_o on a circular plate of radius a and flexural rigidity D with fixed edges,

$$F = \frac{16\pi D}{\left[a^2 - r^2\left(1 + 2\ln\frac{a}{r}\right)\right]} \cdot x \qquad r > r_o \qquad (10)$$

where,

$$D = \frac{h^3 E}{12(1-\upsilon^2)} \qquad (11)$$

where h is thickness, E is Young's modulus and ν is poisson's ratio.

Since the contact radius here is much smaller than the plate radius then it is valid to approximate to a point load at the centre. Hence the load at the plate centre is given by,

$$F = \frac{16\pi D}{a^2} \cdot x \qquad (12)$$

Comparing Equations (7) and (12) gives,

$$k_b = \frac{16\pi D}{a^2} \qquad (13)$$

Which is the same as that given in Shivakumar et al (1985).

This simple model will now be used to develop relationships that normalise for the differences in flexural rigidities of the plates of each material, using the rigidity of the WR plates as a reference value. Since a is constant, equation (13) shows that plate stiffness k_b is proportional to flexural rigidity D.

From equation (6), and since for these tests v_i and M are constant, in order to reduce the impact displacement for direct comparison with that of the WR plate,

$$x_{\max(\text{normalised})} = x_{\max}\sqrt{\frac{D}{D_{WR}}} \qquad (14)$$

Equation (14) may also be used to normalise for x_{end}.

Similarly, from equation (8) for maximum impact force, and since for these tests v_i and M are constant, in order to normalise the maximum force for direct comparison with that of the WR plate,

$$F_{\max(normalised)} = F_{\max}\sqrt{\frac{D_{WR}}{D}} \qquad (15)$$

From equation (9), and since for these tests M is constant, in order to reduce the impact duration for direct comparison with that of the Woven Roving (WR) plate,

$$T_{c(normalised)} = T_c\sqrt{\frac{D}{D_{WR}}} \qquad (16)$$

4 RESULTS

The damage incurred by the GRP specimens is summarised in Table 3 and may be categorised into three main stages:

(i) At very low impact energies the damage was limited to slight permanent indentation and/or matrix cracking.

(ii) At *very low incident energies* an internal delamination suddenly occurred. This delamination then grew and multiple delaminations at different ply interfaces were seen.

(iii) At high incident energies fibre failure occurred (on the back face for thin specimens and on the impacted face for thick specimens), leading to penetration.

Table 3. GRP damage

WR			CSM		
IE (J)	Delamination (mm^2)	Fibre Damage	IE (J)	Delamination (mm^2)	Fibre Damage
Thin Specimens					
1.3	41	-	1	-	-
3.5	219	-	3.4	110	-
5.4	257	-	5.4	177	-
7.5	328	-	7.4	257	i*
10	426	-	10	315	i / b*
15	448	i*	16	358	f / b sp
20	590	i / b*	20	455	f / b sp
31	790	f / b sp	30	400	p
Thick Specimens					
2.7	29	-	2.2	-	-
5.5	152	-	5.8	-	-
11	702	i*	11	870	i*
16	1008	i	15	1106	i
31	1417	f*	30	1466	f*
55	2607	f	55	1876	f
74	2769	f	75	2757	f sp
90	3743	f	90	2782	f sp

f = front-face, b = back-face, i = indent, * = very slight, sp = start of penetration, p = penetration

Typical contact indentation and delamination damage to a CSM laminate are shown Figure 2 (a) and (b) respectively. Further details of the impact damage on marine composites, including the laminates considered here may be found in Sutherland & Guedes Soares (2006).

The metal plates also suffered impact damage at all but the very lowest incident energies. Only 2 specimens, the thin and thick steel plates at 1 and 2J respectively, showed no visible damage. The thick aluminium plate subjected to 2J and the thick steel plate subjected to 5J showed only slight indentation damage under the projectile. All the remaining metal plates suffered both indentation damage (Figure 3a) and plastic deformation of the plate itself (Figure 3b), both of which became more severe with increasing incident energy.

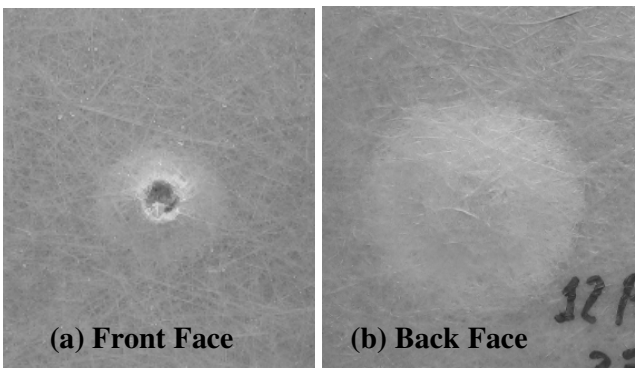

Figure 2. Damage to thick CSM plate (90J)

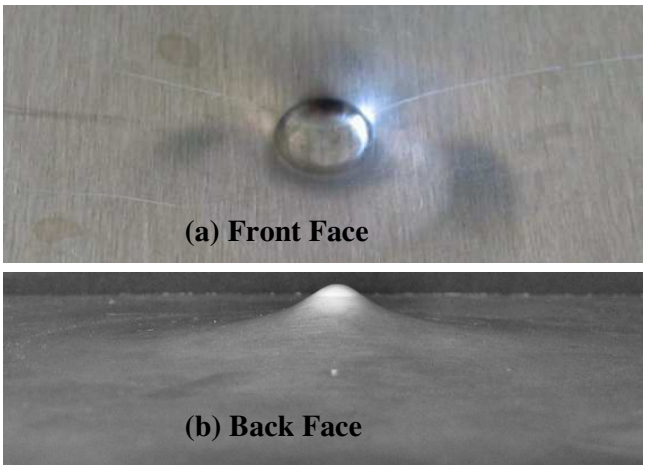

Figure 3. Damage to aluminium thin plate (55J)

In previous work the load cell force data filtered with a low pass filter (second-order discrete Butterworth). However, this often led to a significant phase lag. Hence, the moving average method was used here. Averaging over 5% of the data span resulted in very good filtering with negligible phase lag as can be seen in
Figure 4(a). However, as can be seen in

Figure 4(b), this method did not filter the initial oscillations satisfactorily in some cases when an initial peak was severe (mostly for the thick metal specimens). Despite this, smoothing was used throughout since the advantages of avoiding phase lag were great.
The force-displacement plots for the thin and thick specimens are presented in

Figure 5 and Figure 6 respectively. All tests for that material are shown on each plot, and the incident energies are labelled accordingly.
The impact responses of maximum force, maximum displacement, displacement at end of the impact event and energy irreversibly absorbed are presented in

Figure 7 and Figure 8. Impact durations are given in Figure 9. Where appropriate the values have been normalised, as described in the previous section, to give comparability with the WR results.

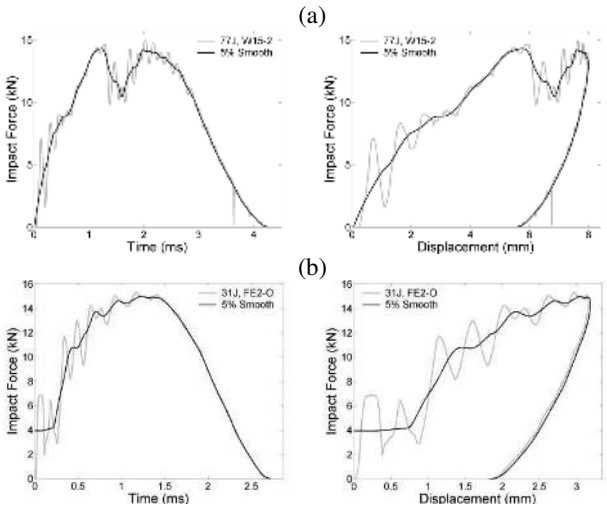

Figure 4. Typical smoothed plots

(a) Thin WR (b) Thin CSM

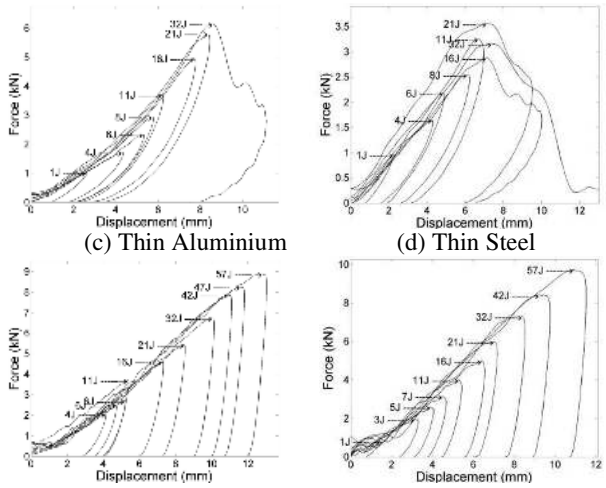

Figure 5: Thin Specimens Force-Displacement Plots

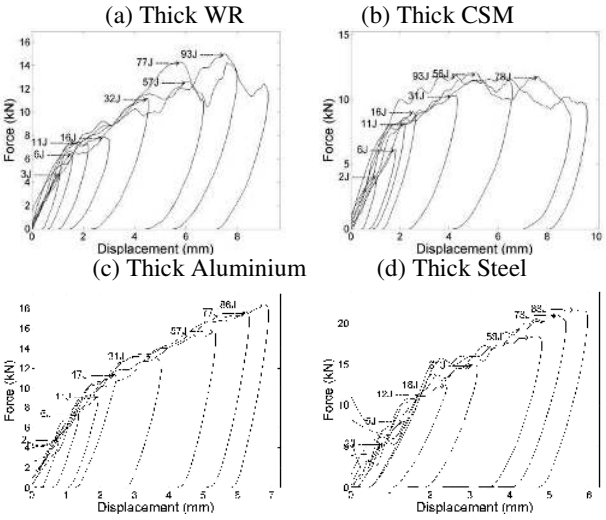

Figure 6: Thick Specimens Force-Displacement Plots

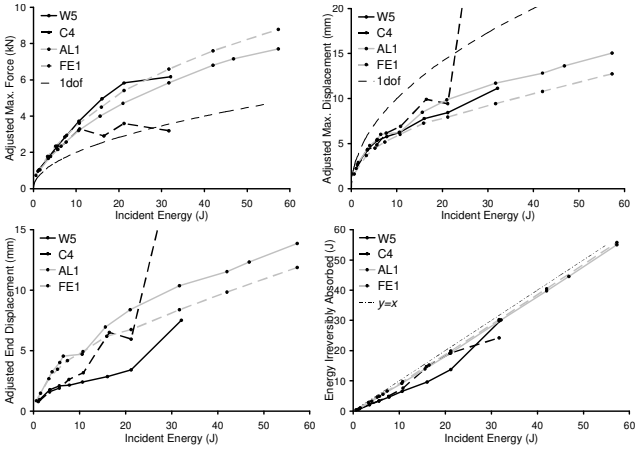

Figure 7: Thin Specimens Results

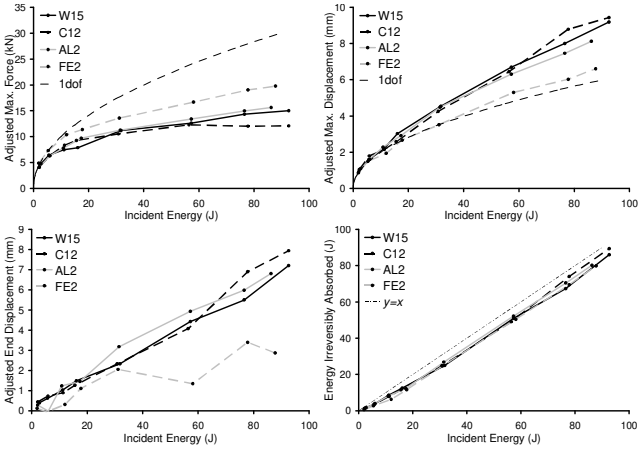

Figure 8: Thick Specimens Results

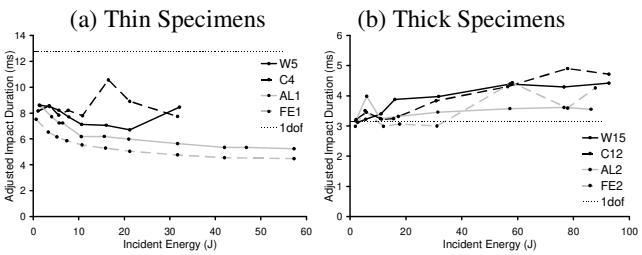

Figure 9: Impact Durations

5 DISCUSSION OF RESULTS

The impact behaviour was seen to be complex, and differed between the thin and the thick plates, and hence these two cases are discussed separately in this section.

5.1 *Thin Plates*

Although the thin composite plates were perforated at higher incident energies, the metal plates were not perforated even at the maximum incident energy attainable by the impact machine with the impact mass used in these tests. However, from the damage seen it was possible to predict that the order of increasing resistance to perforation was CSM, WR, aluminium, steel. Additional tests were also made on 1050 alloy aluminium, which was found to perforate at a much lower incident energy than the 5083 alloy (1050 at 35J, 5083 > 60J). Hence in terms of resistance to perforation, for this impact event, the metal plates outperformed the composite materials considered here.

Only the thin WR plates show a strong non-linear membrane stiffening effect right up to fibre damage (

Figure 5(a)). The metal plates show a slight effect only at low incident energies (

Figure 5(c) and (d)) and the CSM results exhibit linear stiffness ((

Figure 5(b)). However,

Figure 7 and Figure 9 show that compared to the one degree of freedom model (which ignores membrane effects), maximum force is greater and maximum deflection and impact duration are both lower in all cases where there is no perforation. Figure 9 also shows that the impact duration of the metal plates decreases with increasing incident energy. Hence membrane forces are present (which would be expected from the large deflections seen), but their effects have been modified, almost certainly by plastic deformation of the metals, and because the CSM has no continuous fibres to resist such forces and indentation damage is more severe.

The maximum force is very similar for all materials at lower incident energies until fibre failure and perforation causes the CSM values to drop significantly. Plastic deformation leads to lower maximum forces for the metal plates, with the aluminium values lower than those for steel. The WR plates give the highest impact forces of all until fibre damage is suffered.

Very similar maximum displacements are seen for all plates until perforation of the CSM, the order of increasing displacement for the other specimens being aluminium > WR > steel. The final displacement gives some measure of the permanent deformation suffered, a higher value indicating more permanent deformation, and, until fibre damage, this is much lower for the composite materials studied here. When plastic deformation becomes significant, the end displacement of the aluminium becomes greater than that of steel.

It is clear from

Figure 5 that the areas under the curves are much lower in the case of the composite materials, and this is reflected in the absorbed energy values of

Figure 7. Only 60 to 70 percent of the incident energy is irreversibly absorbed by the composite plates as compared to 90 percent for the metal specimens, until fibre damage raises the composite value to 90 percent.

5.2 *Thick Plates*

Figure 6(a) and (b) show the typical bi-linear force-displacement behaviour with a sudden drop in stiffness due to delamination. A reduction in stiffness at higher incident energies for metals is also seen in Figure 6(c) and (d), although this is not as sudden in these cases. This behaviour is thought to be due to local indentation followed by plastic deformation of the plate at higher incident energies.

The maximum forces of Figure 8 follow the one degree of freedom model at low incident energies, but then drop away as indentation fibre damage or plastic deformation occurs. Aluminium and composite plates produce very similar maximum forces, until indentation damage of the CSM becomes significant. The forces on the steel plates are greater than those on the other materials.

The one degree of freedom model predicts well the maximum displacements for steel, and also for the other materials before fibre damage and plastic deformation occur (Figure 8). At higher incident energies the deflections of the aluminium and composite plates are very similar and greater than those of steel plates. The final displacements are very similar for all materials except for the CSM plates which give lower values (Figure 8). This is contrary to what would be expected since Table 3 indicates that these laminates incurred significant indentation damage. This is thought to be because when CSM suffers damage the composite can delaminate causing an increase in laminate thickness.

Figure 8 also shows that the energy absorbed by steel plates at low energies is approximately 50% of the incident energy, but that for the other materials this value is approximately 75% indicating that steel is better at resisting indentation damage. Above an incident energy of approximately 15J, the energy absorbed by all materials is very similar at around 5J less than the incident energy, showing that almost all energy is absorbed by damage.

The impact durations (Figure 9) are generally longer than those predicted by the one degree of freedom, and increase with increasing incident energy due to damage and permanent deformation. However, at very low incident energies the one degree of freedom model predicts well the impact duration, and this model also applies up to approximately 30J for the steel plates.

6 CONCLUSIONS

Comparative data for approximately equal flexural stiffness has been obtained for woven roving and chopped-strand mat glass-polyester laminates, and Aluminium 5083 and steel circular fully-clamped circular plates subjected to central lateral impact with a hemispherical ended dropped weight. The metal plates gave a much higher resistance to perforation than the laminated plates, but the behaviour up to perforation was more complex.

The behaviour with respect to maximum force, maximum deflection, end deflection and absorbed energy are summarised in Table 4. When fibre damage of the composite materials became significant this was accompanied by a corresponding decrease in maximum force and an increase in maximum and final deflections, and absorbed energy.

Table 4: Summary of impact responses

	Thin Plates		Thick Plates	
	Low IE	Higher IE	Low IE	Higher IE
Maximum Force	Little difference	WR>Fe> Al>CSM	Little difference except Fe greater	
Maximum Deflection	Very similar	Fe<WR< Al<CSM	Little difference	Fe lower
Final Deflection	Metals greater	Similar	Similar except CSM lower	
Absorbed Energy	Metals greater	Similar	Fe lower	Little difference

A simple one degree of freedom model was useful in making pertinent comparisons between plates of slightly differing flexural rigidity, but only predicted the impact response for very low incident energies on thick plates.

Both composite material and metal plates suffered damage at very low incident energies. However, the composite delamination damage would not be visible if gel-coated or painted as is normal in practice; the first visible damage would be fibre damage which only occurs at much higher incident energies. Damage to metals is visible even at low incident energies.

Care must be taken to ensure that relevant comparisons are made; flexural stiffness equivalence has been used here, but if strength, thickness, or weight equivalence would have been considered the results would have differed in each case. It is not only material choice but also the plate design that will influence the impact behaviour. For example exchanging steel for GRP based on a stiffness design criterion will give a much thicker plate, and the change in plate thickness may well influence the impact behaviour more than does the change in material.

7 ACKNOWLEDGEMENTS

This work has been performed within the project "MARSTRUCT - Network of Excellence on Marine Structures" (http://www.mar.ist.utl.pt/marstruct/) and has been partially funded by the European Union through the Growth programme under contract TNE3-CT-2003-506141. The first author was financed by the Portuguese Foundation of Science and Technology under the contract number SFRH/BPD/20547/2004.

REFERENCES

Abrate, S. 1998. *Impact on Composite Structures*. Cambridge : Cambridge University Press.

Abrate, S. 2001. Modelling of impacts on composite structures. *Composite Structures* 51: 129–38.

Brewer, T. 1994. *Understanding Boat Design (4th Edition)*. Camden Maine: International Marine.

Du Plessis, H. 1996. *Fibreglass Boats (3rd Edition)*. London: Adlard Coles Nautical.

Gerr, D. 2000. *The Elements of Boat Design*. Camden Maine: International Marine.

Shivakumar KN., Elber W. and Illg W. 1985. Prediction of impact force and duration due to low-velocity impact on circular composite laminates. Journal of Applied Mechanics 52: 674-680.

Sutherland, L. S. & Guedes Soares C. 1999a. Impact tests on woven roving E-glass/polyester laminates. *Composites Science and Technology* 59: 1553-1567.

Sutherland, L. S. & Guedes Soares C. 1999b. Effects of laminate thickness and reinforcement type on the impact behav-

iour of E-glass/polyester laminates. *Composites Science and Technology* 59: 2243-2260.

Sutherland, L. S. & Guedes Soares C. 2003. The effects of test parameters on the impact response of glass reinforced plastic using an experimental design approach. *Composites Science & Technology* 63: 1-18.

Sutherland L.S. & Guedes Soares C. 2004. Effect of laminate thickness and of matrix resin on the impact of low fibre-volume, woven roving E-glass composites. *Composites Science and Technology* 64: 1691-1700.

Sutherland L.S. & Guedes Soares C. 2005a. Impact characterisation of low fibre-volume glass reinforced polyester circular laminated plates. *International Journal of Impact Engineering* 31: 1-23.

Sutherland, L. S. & Guedes Soares C. 2005b. Impact on low fibre-volume, glass / polyester rectangular plates. *Composites Structures* 68: 13–22.

Sutherland, L. S. & Guedes Soares C. 2005c. Contact indentation of marine composites. *Composites Structures* 70(3): 287-294.

Sutherland, L. S. & Guedes Soares C. 2006. Impact behaviour of typical marine composite laminates. *Composites Part B: Engineering* 37(2-3): 89-100.

Sutherland, L. S. & Guedes Soares C. 2007. Scaling of impact on low fibre-volume glass-polyester laminates. *Composites Part A: Applied Science and Manufacturing* 38: 307-317.

Trower, G. 1999. *Yacht and Small Craft Construction: Design Decisions*. Marlborough Wiltshire: Crowood Press.

Young, W. C. 1989. *Roark's Formulas for Stress and Strain*. Singapore: McGraw-Hill.